Metal−Metal Multiply Bonded Complexes of Technetium. 5.[1] Tris and Tetrakis(formamidinato) Complexes of Ditechnetium

F. Albert Cotton,*,† Steven C. Haefner,†,‡,§ and Alfred P. Sattelberger*,‡

Chemical Science and Technology Division, Los Alamos National Laboratory, Los Alamos, New Mexico 87545, and the Laboratory for Molecular Structure and Bonding, Department of Chemistry, Texas A&M University, College Station, Texas 77843

Received May 16, 1996[⊗]

Compounds of the type $Tc_2Cl_4(PR_3)_4$ (PR_3 = PEt_3, PMe_2Ph, $PMePh_2$) react with the molten formamidines HDPhF (HDPhF = diphenylformamidine) and HDTolF (HDTolF = di-*p*-tolylformamidine) to produce mixtures of tris- and tetrakis-bridged formamidinate complexes of ditechnetium. The displacement of chloride and phosphine by $[DPhF]^-$ was accompanied by the oxidation of the dimetal core to produce the mixed-valent complexes $Tc_2(DPhF)_3Cl_2$ (**1**) and $Tc_2(DPhF)_4Cl$ (**2**) in modest yield. The solid-state structures of the di-*p*-tolyl analog of **1**, $Tc_2(DTolF)_3Cl_2$ (**1a**), and $Tc_2(DPhF)_4Cl{\cdot}C_7H_8$ (**2**·C_7H_8) have been determined by single crystal X-ray diffraction studies and are described in detail. The structure of **1a** consists of three formamidinate ligands spanning the two technetium atoms. The two chloride ligands, which complete the coordination sphere, are bound equatorially at distances of 2.357(1) and 2.346(2) Å from the metals. Though possessing no crystallographic symmetry, **1a** approximates C_{2v} symmetry. The metal−metal bond length of 2.0937(6) Å ranks among the shortest reported for technetium and is indicative of a Tc−Tc multiple bond. Compound **2** crystallizes with the Tc atoms colinear with a crystallographic 4-fold axis. The four bridging formamidinate ligands are arranged in a lantern geometry about the dimetal unit. The chloride is bonded in an axial position at a distance of 2.450(4) Å. The Tc−Tc bond length of 2.119(2) Å is also consistent with the presence of a high order Tc−Tc bond. The electronic structures of **1** and **2** were investigated by means of SCF−Xα−SW molecular orbital calculations using the model compounds $Tc_2(HNCHNH)_3Cl_2$ and $Tc_2(HNCHNH)_4Cl$. The results support the presence of a $\sigma^2\pi^4\delta^2\delta^*$ ground state configuration giving rise to a formal bond order of 3.5. The LUMO in both cases is a low-lying π^* orbital. The formamidinate complexes **1** and **2** have been further characterized by IR spectroscopy and cyclic voltammetry. The crystallographic parameters for **1a** and **2**·C_7H_8 are as follows: $Tc_2(DTolF)_3Cl_2$ (**1a**), monoclinic space group $P2_1/n$ (No. 14) with a = 16.185(2) Å, b = 15.637(2) Å, c = 17.812(1) Å, β = 110.142(5)°, V = 4232.3(6) Å^3 and Z = 4; $Tc_2(DPhF)_4Cl{\cdot}C_7H_8$ (**2**·C_7H_8), tetragonal space group $P4/ncc$ (No. 130) with a = 15.245(2) Å, c = 21.832(3) Å, V = 5074.1(9) Å^3 and Z = 4.

Introduction

While the field of metal−metal multiple-bond chemistry has progressed at a dramatic pace over the last twenty years, our knowledge about Tc−Tc systems remains rather limited.[2] In large part, this is due to the inherent radioactivity of all isotopes of Tc. Its radioactivity has limited the ability of many laboratories to study the chemistry of this fascinating element. The work that has been performed has focused on the applications of the ^{99m}Tc isotope in diagnostic imaging agents.[3] As a result of this emphasis, the development of ditechnetium complexes that possess metal−metal multiple bonds has advanced slowly.

Progress in this field has been further impeded by the limited availability of suitable starting materials for the exploration of ditechnetium chemistry. The subtle differences between the chemistry of technetium and its third row congener rhenium prevent a simple carry over of the synthetic methodology already established for the preparation of dirhenium complexes. This point is dramatically illustrated by the differences between the preparation and stability of the Tc and Re octahalide species $[M_2X_8]^{n-}$, the primary pathway into Re−Re multiple-bond chemistry.[2] Only recently have synthetic methods been reported for higher yield preparations of $[Tc_2Cl_8]^{3-,2-}$.[4] We have developed an entirely different approach to the preparation of Tc−Tc multiply bonded compounds, one that avoids the intermediacy of the octahalide species. As a result of these efforts, we have established a high yield synthetic route to the preparation of $Tc_2Cl_4(PR_3)_4$ (PR_3 = PEt_3, $P(n\text{-}Pr)_3$, PMe_2Ph, and $PMePh_2$) using readily available mononuclear precursors.[1a] These Tc(II)−Tc(II) species represent the first discrete ditechnetium complexes with an electron-rich triple bond. Their ease of preparation combined with their relative stability under a variety of reaction conditions make them ideal precursors for the synthesis of new metal−metal multiply bonded complexes of technetium. Specifically, $Tc_2Cl_4(PR_3)_4$ (PR_3 = PEt_3, PMe_2Ph

† Texas A&M University.
‡ Los Alamos National Laboratory.
§ Present address: Department of Chemistry, Wake Forest University, Winston-Salem, NC 27109-7486.
⊗ Abstract published in *Advance ACS Abstracts,* October 15, 1996.

(1) (a) Part 1: Burns, C. J.; Burrell, A. K.; Cotton, F. A.; Haefner, S. C.; Sattelberger, A. P. *Inorg. Chem.* **1994**, *33*, 2257. (b) Part 2: Bryan, J. C.; Cotton, F. A.; Daniels, L. M.; Haefner, S. C.; Sattelberger, A. P. *Inorg. Chem.* **1995**, *34*, 1875. (c) Part 3: Cotton, F. A.; Haefner, S. C.; Sattelberger, A. P. *Inorg. Chem.* **1996**, *35*, 1841. (d) Part 4: Cotton, F. A.; Haefner, S. C.; Sattelberger, A. P. *J. Am. Chem. Soc.* **1996**, *118*, 5486.
(2) Cotton, F. A.; Walton, R. A. *Multiple Bonds Between Metal Atoms*, 2nd ed; Oxford University Press: Oxford, U.K., 1993 and references therein.
(3) (a) Schwochau, K. *Angew. Chem., Int. Ed. Engl.* **1994**, *33*, 2258. (b) Jurrison, S.; Berring, D.; Jia, W.; Ma, D. *Chem. Rev.* **1993**, *93*, 1137. (c) Steigman, I.; Eckelman, W. C. *The Chemistry of Technetium in Medicine*; National Academy Press: Washington, D.C., 1992. (d) Deutsch, E.; Libson, K.; Jurisson, S.; Lindroy, L. F. *Prog. Inorg. Chem.* **1983**, *30*, 75.
(4) Preetz, W.; Peters, G.; Bublitz, D. *J. Cluster Sci.* **1994**, *5*, 83 and references therein.

S0020-1669(96)00535-6 CCC: $12.00

Group 5	Group 6	Group 7	Group 8	Group 9	Group 10
V_2^{4+} [5]	Cr_2^{4+} [6]	Mn	Fe_2^{4+} [7]	Co_2^{4+} [8]	Ni_2^{4+} Ni_2^{5+} [9]
Nb	Mo_2^{4+} Mo_2^{5+} [10]	Tc	Ru_2^{4+} Ru_2^{5+} Ru_2^{6+} [11]	Rh_2^{4+} Rh_2^{5+} [12]	Pd_2^{4+} Pd_2^{5+} [13]
Ta	W_2^{4+} [6]	Re_2^{4+} Re_2^{5+} Re_2^{6+} [14]	Os_2^{6+} [15]	Ir_2^{4+} [16]	Pt_2^{4+} Pt_2^{5+} [17]

Figure 1. Diagram showing those dimetal cores for which tetrakis(amidinate) complexes of the type $M_2(RNCR'NR)_4X_n$ (n = 0, 1, 2) exist. Shaded boxes represent metals for which the dimetal tetrakis(amidinate) species are as yet unknown. The appropriate literature citations appear within brackets.

and $PMePh_2$) may be acidified with $HBF_4 \cdot Et_2O$ in acetonitrile to produce the fully solvated ditechnetium cation $[Tc_2(CH_3CN)_{10}]^{4+}$ in good yield.[1b] Additionally, $Tc_2Cl_4(PMe_2Ph)_4$ is readily oxidized by one electron to produce the mixed-valence species $[Tc_2Cl_4(PMe_2Ph)_4][PF_6]$ and $Tc_2Cl_5(PMe_2Ph)_3$.[1c] As a continuation of this work, we have investigated the use of $Tc_2Cl_4(PR_3)_4$ as a synthon for the preparation of the first amidinato complexes of ditechnetium.

The use of amidinate ligands, cousins of the ubiquitous carboxylate ligands, has become increasingly prominent in the area of metal−metal multiple-bond research. Reports by this laboratory and others have established amidinate ligands as a widely useful support for the stabilization of metal−metal bonds (see Figure 1). The ability of this ligand to stabilize different oxidation states of the same bimetallic core has provided valuable information regarding the electronic structure of many metal−metal multiply bonded complexes. Amidinate ligands have been particularly effective at fostering metal−metal bonding interactions between first row transition metal ions as evidenced by the preparation of the first metal−metal multiply bonded complexes of the V_2^{2+} and Fe_2^{4+} cores using a tetrakis(formamidinate) framework.[5,7] Their success derives from their enhanced π-basicity which allows for the stabilization of several dimetal cores in two or three different oxidation states.[18]

From Figure 1 it can be seen that tetrakis(formamidinate) complexes exist for nearly every transition metal from group 5 to group 10. The exceptions are technetium and manganese in group 7, as well as niobium and tantalum in group 5. Given the central position of technetium in the transition metal series, it seemed highly probable that a tetrakis(formamidinate) complex could be readily prepared. Herein we describe the isolation and solid state structures of $Tc_2(DPhF)_4Cl$ (DPhF = *N*,*N*′-diphenylformamidinate), as well as the novel tris(formamidinate) complex $Tc_2(DTolF)_3Cl_2$ (DTolF = N,N′-di-*p*-tolylformamidinate).[19] The results of molecular orbital calculations using the SCF−Xα−SW method on the model complexes $Tc_2(HNCHNH)_3Cl_2$ and $Tc_2(HNCHNH)_4Cl$ are also presented.

Experimental Section

General Considerations. *Caution!* The isotope ^{99}Tc is a low-energy β-emitter (E_{max} = 0.29 MeV) with a half-life of 2.1×10^5 years. All manipulations were carried out in laboratories approved for low-level radioactive materials following procedures and techniques described elsewhere.[20] Ammonium pertechnetate was obtained from Oak Ridge National Laboratory and was purified as described previously.[21] $Tc_2Cl_4(PR_3)_4$ (PR_3 = PEt_3, PMe_2Ph and $PMePh_2$) was prepared following literature procedures.[1a] Reagents were purchased from commercial sources and used without further purification. Toluene, hexanes, THF, and diethyl ether were distilled under N_2 from either sodium or sodium/potassium alloy. Acetonitrile and methylene chloride were distilled under N_2 from CaH_2. Unless noted otherwise, the transfer of air-sensitive solids and the workup of air-sensitive reaction mixtures were carried out within the confines of a Vacuum Atmospheres Co. glove box equipped with a Dri-Cold freezer maintained at −40 °C.

Preparation of $Tc_2(DPhF)_3Cl_2$ (1). $Tc_2Cl_4(PEt_3)_4$ (0.10 g, 0.12 mmol) and an excess of HDPhF (0.60 g, 3.06 mmol) were heated to 140 °C using an oil bath. Once the formamidine had melted, a vacuum was applied to the reaction slurry in order to remove HCl and PEt_3. After being heated under vacuum for 3 h, the flask was allowed to cool to room temperature leaving a red-purple residue. Then 5 mL of acetonitrile was added to the residue, producing a reddish brown solution with an undissolved crystalline solid. The red-purple solid was collected by filtration, washed with copious amounts of diethyl ether, and dried under vacuum; yield 0.052 g (51%). IR (Nujol, cm^{-1}): 1592 (m), 1584 (m), 1534 (s), 1488 (s), 1316 (s), 1220 (s), 1189 (w), 1174 (w), 1159 (w), 1077 (w), 1027 (w), 940 (m), 908 (w), 900 (w), 776 (w), 767 (m), 755 (s), 727 (w), 697 (s), 687 (s), 513 (m), 437 (m). Electronic absorption spectrum (λ_{max}, CH_2Cl_2, nm): 504, 405, 348, 278. CV (200 mV/s, CH_2Cl_2, TBAH): $E_{1/2,\ ox}$ = −0.2 V, $E_{1/2,\ red}$ = −1.5 V vs Cp_2Fe. Use of $Tc_2Cl_4(PR_3)_4$ (PR_3 = $PMePh_2$, PMe_2Ph) as a precursor gave similar results. The tolyl derivative $Tc_2(DTolF)_3Cl_2$ (**1a**) was prepared in a similar manner, but with a much lower overall yield. Single crystals of **1a** were grown by slow diffusion of a layer of hexanes into a solution of **1a** in methylene chloride.

Preparation of $Tc_2(DPhF)_4Cl$ (2). A mixture of $Tc_2Cl_4(PMePh_2)_4$ (0.2 g, 0.17 mmol) and HDPhF (0.70 g, 3.6 mmol) were placed in a 50 mL round bottom flask with a Teflon-coated stir bar and heated to 150−160 °C using an oil bath. Once the formamidine began to melt, a vacuum was applied to the reaction mixture. The reaction mixture was heated under vacuum for 2 h. After cooling, the resulting dark-colored residue was washed repeatedly with toluene to remove excess HDPhF. The solid was extracted with 5 × 5 mL of thf. The thf extracts were then concentrated to approximately 5 mL and 2−3 mL of toluene was slowly added. The solvent mixture was concentrated further to produce a red solid. The solid was collected by filtration, washed with

(5) (a) Cotton, F. A.; Daniels, L. M.; Murillo, C. A. *Angew. Chem., Int. Ed. Engl.* **1992**, *31*, 737. (b) Cotton, F. A.; Daniels, L. M.; Murillo, C. A. *Inorg. Chem.* **1993**, *32*, 2881.
(6) Cotton, F. A.; Ren, T. *J. Am. Chem. Soc.* **1992**, *114*, 7195.
(7) Cotton, F. A.; Daniels, L. M.; Murillo, C. A. *Inorg. Chim. Acta* **1994**, *224*, 5.
(8) He, L.-P.; Yao, C.-L.; Naris, M.; Lee, J. C.; Korp; J. D.; Bear, J. L. *Inorg. Chem.* **1992**, *31*, 620.
(9) Cotton, F. A.; Matusz, M.; Poli R.; Feng, X. *J. Am. Chem. Soc.* **1988**, *110*, 1144.
(10) (a) Cotton, F. A.; Feng; X.; Matusz, M. *Inorg. Chem.* **1989**, *28*, 594. (b) Cotton, F. A.; Inglis, T.; Kilner, M.; Webb, T. R. *Inorg. Chem.* **1975**, *14*, 2023. (c) Lin, C.; Protasiewicz, J. D.; Smith, E. T.; Ren, T. *J. Chem Soc., Chem. Commun.* **1995**, 2257.
(11) (a) Cotton, F. A.; Ren, T. *Inorg. Chem.* **1995**, *34*, 3190. (b) Cotton, F. A.; Ren, T. *Inorg. Chem.* **1991**, *30*, 3675. (c) Bear, J. L.; Han, B.; Huang, S. R. *J. Am. Chem. Soc.* **1993**, *115*, 1175. (d) Li, Y.-L.; Han, B. C.; Bear, J. L. *Inorg. Chem.* **1993**, *32*, 4175.
(12) (a) Bear, J. L.; Yao, C.-L.; Lifsey, R. S.; Korp, J. D.; Kadish, K. M. *Inorg. Chem.* **1991**, *30*, 336. (b) Piraino, P.; Bruno, G.; Schiavo, S. L.; Laschi, F.; Zanello, P. *Inorg. Chem.* **1987**, *26*, 2205. (c) Le, J. C.; Chavan, M. Y.; Chou, L. K.; Bear, J. L.; Kadish, K. M. *J. Am. Chem. Soc.* **1985**, *107*, 7195.
(13) Yao, C.-L.; He, L.-P.; Korp, J. D., Bear, J. L. *Inorg. Chem.* **1988**, *27*, 4389.
(14) Cotton, F. A.; Ren, T. *J. Am. Chem. Soc.* **1992**, *114*, 2495.
(15) Cotton, F. A.; Ren, T.; Eglin, J. L. *Inorg. Chem.* **1991**, *30*, 2559.
(16) Cotton, F. A.; Poli, R. *Polyhedron* **1987**, *6*, 1625.
(17) Cotton, F. A.; Matonic, J. H.; Murillo, C. A. *Inorg. Chem.* **1996**, *35*, 498.
(18) Barker; J.; Kilner, M. *Coord. Chem. Rev.* **1994**, *133*, 219.
(19) The nomenclature used is that developed previously: Cotton, F. A.; Daniels, L. M.; Maloney, D. J.; Matonic, J. H.; Murillo, C. A. *Polyhedron* **1994**, *13*, 815.
(20) Bryan, J. C.; Burrell, A. K.; Miller, M. M.; Smith, W. H.; Burns, C. J.; Sattelberger, A. P. *Polyhedron* **1993**, *12*, 1769.
(21) Libson, K.; Barnett, B. L.; Deutsch, E. *Inorg. Chem.* **1983**, *22*, 1695.

Table 1. Crystallographic Data for $Tc_2(DTolF)_3Cl_2$ (**1a**) and $Tc_2(DPhF)_4Cl{\cdot}C_7H_8$ (**2**·C_7H_8)

	1a	**2**·C_7H_8
formula	$C_{45}H_{45}Cl_2N_6Tc_2$	$C_{59}H_{52}Cl_1N_8Tc_2$
fw	936.77	1104.54
space group	$P2_1/n$ (No. 14)	$P4/ncc$ (No. 130)
a, Å	16.185(2)	15.245(2)
b, Å	15.637(2)	
c, Å	17.812(1)	21.832(2)
β, deg	110.142(5)	
V, Å^3	4232.3(6)	5074.1(9)
Z	4	4
ρ_{calc}, g/cm^3	1.470	1.446
μ, cm^{-1}	67.66 (Cu Kα)	52.79 (Cu Kα)
transmission coeff, max−min	1.00−0.70	1.00−0.75
radiation (monochromated in incident beam)	Cu Kα ($\lambda_\alpha = 1.5406$)	Cu Kα ($\lambda_\alpha = 1.5406$)
temp, °C	23 ± 2	23 ± 2
R^a ($I > 2\sigma(I)$)	0.045	0.048
$R_w{}^{b,c}$ ($I > 2\sigma(I)$)	0.117	0.125
quality-of-fit-indicator^{c,d}	1.10	1.09

^{a} $R = \sum||F_o| - |F_c||/\sum|F_o|$. ^{b} $R_w = [\sum[w(F_o^2 - F_c^2)^2]/\sum[w(F_o^2)^2]]^{1/2}$. ^{c} Weight $= 1/[\sigma(F_o^2)^2 + (aP)^2 + (bP)]$, where $P = [\max(F_o,^20) + 2F_c^2]/3$. ^{d} Quality of fit $= [\sum[w(F_o^2 - F_c^2)^2]/(N_{obs} - N_{param})]^{1/2}$; based on all data.

diethyl ether, and dried in vacuo; yield 0.035 g (20%). IR (Nujol, cm^{-1}): 1592 (m), 1579 (m), 1533 (s), 1518 (s), 1487 (s), 1411 (m), 1313 (s), 1304 (s), 1220 (s), 1155 (w), 1079 (w), 1029 (w), 1011 (w), 938 (w), 899 (m), 865 (w), 774 (m), 761 (m), 729 (s), 697 (s), 658 (w), 518 (w), 466 (w), 438 (w). CV (200 mV/s, CH_2Cl_2, TBAH): $E_{1/2,ox} = -0.46$ V, $E_{1/2,red} = -1.73$ V vs Cp_2Fe. Similar yields were obtained using either $Tc_2Cl_4(PEt_3)_4$ or $Tc_2Cl_4(PMe_2Ph)_4$. Single crystals suitable for X-ray diffraction studies were obtained by slow evaporation of a solution of **2** in a mixture of methylene chloride and toluene.

Physical Measurements. Infrared spectral data were obtained as Nujol mulls on KBr plates using a Bio Rad FTS-40 spectrophotometer. Electronic absorption spectra were measured on a Perkin-Elmer λ9 UV/IR spectrophotometer. Electrochemical measurements were performed on an EG&G Princeton Applied Research Model 273 potentiostat. Cyclic voltammetry experiments were carried out at room temperature in CH_2Cl_2 using 0.1 M [n-Bu_4N][BF_4] as a supporting electrolyte. A platinum disk working electrode and a platinum wire counter electrode were used in conjunction with a silver wire quasi-reference electrode that was separated from the bulk solution by a fine porosity glass frit. $E_{1/2}$ values, determined as $(E_{p,a} + E_{p,c})/2$, are reported relative to an internal ferrocene standard.

X-ray Crystallographic Procedures. Crystallographic data for $Tc_2(DTolF)_3Cl_2$ (**1a**) and $Tc_2(DPhF)_4Cl{\cdot}C_7H_8$ (**2**·C_7H_8) were collected following well-established procedures that have been fully described elsewhere.[22] All calculations were performed on a local area VMS cluster at Texas A&M University employing a VAX/VMS 6.1 computer. Data were corrected for Lorentz and polarization effects. Structure refinement was carried out using SHELXL-93.[23] Crystallographic parameters and basic information pertaining to data collection and structure refinement are summarized in Table 1. Selected bond distances and angles are listed in Tables 2 and 3. Tables of anisotropic displacement parameters as well as complete tables of bond distances and angles are available as Supporting Information.

$Tc_2(DTolF)_3Cl_2$ (1a). Red-purple, block-shaped crystals of **1a** were obtained by slow evaporation of a solution of **1a** in CH_2Cl_2 and heptane. A well shaped single crystal with approximate dimensions of 0.4 × 0.3 × 0.2 mm^3 was selected and mounted with epoxy cement onto the tip of a glass fiber. Intensity measurements were made at ambient temperature on a Rigaku AFC5R diffractometer equipped with a rotating Cu radiation source ($\lambda_{Cu\alpha} = 1.540\,598$ Å). Indexing and least-squares refinement of 25 well-centered reflections in the range $60 \le 2\theta \le 90°$ yielded lattice parameters consistent with a primitive monoclinic cell. The lattice parameters and symmetry were confirmed via axial photography. Using a $\theta-2\theta$ scan technique, a total of 6545 data were collected in the range $6 \le 2\theta \le 120°$. Averaging of equivalent reflections left 6295 unique reflections of which 5095 were considered observed with $F_o^2 > 2\sigma(F_o^2)$. Routine monitoring of 3 standard reflections revealed a 15% decay in intensity that was accounted for by the application of a linear decay correction. An absorption correction was applied to data based on azimuthal scans of several reflections near $\chi = 90°$. Examination of the systematic absences led to the selection of the space group $P2_1/n$ as the crystallographic space group. The positions of the Tc atoms were determined by direct methods.[24] The remaining non-hydrogen atoms were subsequently located through an alternating series of least-squares cycles and Fourier difference maps. Hydrogen atoms were placed at calculated positions and allowed to ride on the associated carbon atom with their thermal parameters proportional to those of the carbon atoms. All non-hydrogen atoms were refined with anisotropic displacement parameters. Final least-squares refinement of 496 parameters produced residuals R (based on F) and R_w (based on F^2) of 0.045 and 0.117 respectively.[25] The largest remaining peak in the difference map was 0.70 e/Å^3 and the quality-of-fit based on F^2 for all data was 1.10.

$Tc_2(DPhF)_4Cl{\cdot}C_7H_8$ (2·C_7H_8). A red orange plate-like crystal was selected and mounted with epoxy cement on the tip of a glass fiber. Data collection was performed at ambient temperature on a Rigaku

Table 2. Selected Bond Distances (Å) and Angles (deg) for $Tc_2(DTolF)_3Cl_2$ (**1a**)

Tc(1)−Tc(2)	2.0937(6)	Tc(1)−Cl(1)	2.357(1)
Tc(1)−N(1)	2.093(5)	Tc(1)−N(3)	2.092(5)
Tc(1)−N(5)	2.068(5)	Tc(2)−Cl(2)	2.346(2)
Tc(2)−N(2)	2.091(5)	Tc(2)−N(4)	2.121(5)
Tc(2)−N(6)	2.108(5)	N(1)−C(1)	1.324(7)
N(2)−C(1)	1.315(7)	N(3)−C(16)	1.312(8)
N(4)−C(16)	1.328(8)	N(5)−C(31)	1.334(7)
N(6)−C(31)	1.318(8)		
Tc(2)−Tc(1)−Cl(1)	108.80(4)	N(2)−Tc(2)−N(4)	173.2(2)
N(3)−Tc(1)−N(1)	175.2(2)	N(6)−Tc(2)−N(4)	92.9(2)
N(5)−Tc(1)−N(1)	87.1(2)	N(2)−Tc(2)−Cl(2)	86.0(1)
N(5)−Tc(1)−N(3)	91.8(2)	N(6)−Tc(2)−Cl(2)	160.8(1)
N(1)−Tc(1)−Tc(2)	92.7(1)	N(4)−Tc(2)−Cl(2)	89.1(1)
N(3)−Tc(1)−Tc(2)	92.0(1)	C(1)−N(1)−Tc(1)	116.5(4)
N(5)−Tc(1)−Tc(2)	94.6(1)	C(1)−N(2)−Tc(2)	117.3(4)
N(1)−Tc(1)−Cl(1)	88.8(1)	C(16)−N(3)−Tc(1)	118.3(4)
N(3)−Tc(1)−Cl(1)	90.6(1)	C(16)−N(4)−Tc(2)	115.2(4)
N(5)−Tc(1)−Cl(1)	156.4(1)	C(31)−N(5)−Tc(1)	115.9(4)
N(2)−Tc(2)−Tc(1)	92.5(1)	C(31)−N(6)−Tc(2)	117.8(4)
N(2)−Tc(2)−N(6)	90.3(2)	N(2)−C(1)−N(1)	120.4(6)
Tc(1)−Tc(2)−Cl(2)	107.94(5)	N(3)−C(16)−N(4)	120.9(6)
Tc(1)−Tc(2)−N(4)	93.5(1)	N(6)−C(31)−N(5)	120.2(6)
Tc(1)−Tc(2)−N(6)	91.0(1)		

Table 3. Selected Bond Distances (Å) and Angles (deg) for $Tc_2(DPhF)_4Cl{\cdot}C_7H_8$ (**2**·C_7H_8)

Tc(1)−Tc(2)	2.119(2)	Tc(2)−Cl(1)	2.450(4)
Tc(1)−N(1)	2.075(7)	N(1)−C(1)	1.341(9)
Tc(2)−N(2)	2.147(6)	N(2)−C(1)	1.318(9)
Tc(1)−Tc(2)−N(2)	89.3(2)	Tc(1)−Tc(2)−Cl(1)	180.0
N(1)−Tc(1)−N(1)′	89.65(3)	N(2)−Tc(2)−Cl(1)	90.7(2)
N(1)−Tc(1)−N(1)†	171.0(3)	C(1)−N(1)−Tc(1)	115.6(5)
N(1)−Tc(1)−Tc(2)	94.5(2)	C(1)−N(2)−Tc(2)	117.5(5)
N(2)−Tc(2)−N(2)″	89.993(4)	N(2)−C(1)−N(1)	120.2(7)
N(2)−Tc(2)−N(2)†	178.6(3)		

^{a} Symmetry transformations used to generate equivalent atoms: ′ $y, -x + {}^1/_2, z$; ″ $-y + {}^1/_2, x, z$; † $-x + {}^1/_2, -y + {}^1/_2, z$.

(22) (a) Bino, A.; Cotton, F. A.; Fanwick, P. E. *Inorg. Chem.* **1979**, *18*, 3558. (b) Cotton, F. A.; Frenz, B. A.; Deganello, G.; Shaver, A. *J. Organomet. Chem.* **1979**, *50*, 227.

(23) SHELXL-93: Sheldrick, G. M. In *Crystallographic Computing 6*; Flack, H. D., Parkanyi, L., Simon, K., Eds.; Oxford University Press: Oxford, U.K., 1993; pp 111−122.

(24) SHELXS-86: Sheldrick, G. M. In *Crystallographic Computing 3*; Sheldrick, G. M., Kruger, C., Goddard, R., Eds.; Oxford University Press: Oxford, U.K., 1985; pp 175−189.

(25) R factors based on F^2 are statistically about twice as large as those based on F, and an R-index based on all data is inevitably larger than one based only on data with F greater than a given threshold.

AFC5R diffractometer equipped with a rotating Cu radiation source ($\lambda_{Cu\alpha}$ = 1.541 84 Å). Cell parameters consistent with a primitive tetragonal lattice were obtained by least-squares refinement of 25 well-centered reflections in the range $18 \leq 2\theta \leq 36°$. The unit cell dimensions and the 4/*mmm* Laue symmetry were confirmed by axial photography. Periodic monitoring of three representative reflections revealed a 1.7% loss of diffraction intensity. The observed decay was corrected by application of a linear decay correction. An absorption correction based on azimuthal scans of several reflections near $\chi = 90°$ was applied to data. A total of 1897 data in the range $8 < 2\theta < 120$ were collected using a $\theta-2\theta$ scan technique. Of these data, 944 were considered observed with $F_o^2 > 2\sigma(F_o^2)$. Examination of systematic absences and intensity statistics led to the selection of space group *P*4/*ncc*. This choice was latter confirmed through successful least-squares refinement. The position of the Tc atom was determined by direct methods.[24] The remaining non-hydrogen atoms were located from a series of alternating least-squares cycles and difference Fourier maps. After initial isotropic refinement of the molecular species, a disordered toluene molecule was located from the difference map. The toluene molecule resides on the intersection of two 2-fold axes creating two separate orientations for the molecule. One crystallographic C_2 axis passes through the two carbon atoms (C(15) and C(15)′) *ortho* to the methyl group, while the second axis bisects the molecule through the methyl, *ipso*, and *para* carbon atoms. The presence of the 2-fold axis passing through the *ortho*-positions causes C(16) to occupy the methyl position for one orientation and the *para* position for the second orientation. C(14) and C(17) participate in only one orientation at a time and were therefore refined at half-occupancy. The carbon atoms in the disordered group were restrained to be approximately coplanar, and their thermal displacement parameters were restrained to be similar. All non-hydrogen atoms were refined with anisotropic thermal parameters. Hydrogen atoms were included at calculated positions with their thermal parameters proportional to those of the associated carbon atom. Those hydrogen atoms associated with the disordered toluene molecule were, however, not included in the structure factor calculation. Final least-squares refinement of 169 parameters converged with R (based on F) of 0.048 and R_w (based of F^2) of 0.125.[25] The quality-of-fit for all data based on F^2 was 1.1. The largest remaining peak in the final difference map, which was located 1.0 Å from Tc(2), was 0.4 e/Å^3.

Computational Procedures. Molecular orbital calculations on the model complexes $Tc_2(HNCHNH)_3Cl_2$ (**1m**) and $Tc_2(HNCHNH)_4Cl$ (**2m**) were carried out using the SCF−Xα−SW method.[26] The atomic coordinates used for the calculations were taken from crystallographic data for **1a** and **2** and idealized to C_{2v} and C_{4v} symmetry, respectively. The coordinate system used for both calculations was one in which the *z* axis was colinear with the Tc−Tc bond. For $Tc_2(HNCHNH)_3Cl_2$ the *x* axis was directed toward the unique formamidinate ligand. The idealized structural parameters used in the calculations are as follows: $Tc_2(HNCHNH)_4Cl$, Tc1−Tc2 = 2.12 Å, Tc−Cl = 2.45 Å, Tc1−N1 = 2.08 Å, Tc2−N2 = 2.15 Å, N1−C = 1.33 Å, N2−C = 1.33 Å, N1−C−N2 = 120°; $Tc_2(HNCHNH)_3Cl_2$, Tc−Tc′ = 2.09 Å, Tc−Cl = 2.35 Å, Tc−N_x = 2.09 Å, N_x−C_x = 1.33 Å, N_x−C_x−N_x′ = 120°. Tc−N_y = 2.10 Å, N_y−C_y = 1.32 Å, N_y−C_y−N_y′ = 120°, Tc′−Tc−Cl = 108°, Tc′−Tc−N = 93°. In both models the bond lengths used for C−H and N−H were 1.08 and 1.06 Å, respectively.

The initial molecular potentials were constructed from Herman−Skillman atomic potentials and the H 1s radial wave function.[27] The atomic radii were taken as 89% of the Norman atomic number radii.[28] The resulting atomic spheres were allowed to overlap. In both calculations, the outer-sphere radii were chosen tangential to the outermost atomic sphere. Schwarz's α atomic exchange parameters were used with valence-electron weighted average of the atomic α values for the inter- and outer-sphere regions.[29]

Results and Discussion

Synthesis. The reaction of dimetal tetracarboxylates with excess molten ligand has proven to be an effective method for the preparation of tetrakis(formamidinate) compounds such as $M_2(DTolF)_4Cl_2$ (M = Re,[14] Os[15]) and $Ru_2(DTolF)_4Cl$,[11a] as well as several hydroxypyridinate and amidate complexes.[30] Although formamidines and hydroxypyridines are less acidic than carboxylic acids, the carboxylate ligand, when protonated, is driven out of solution because of its volatility at the elevated temperatures used to melt the ligand. Likewise, we reasoned that complexes of the type $M_2Cl_4(PR_3)_4$ might behave in a similar fashion. We expected that the volatility of PR_3 and HCl(g), produced by transfer of H^+ from the formamidine to the Cl^-, could be harnessed as a driving force to push the equilibrium toward the formation of a formamidinate complex. Indeed, compounds of the type $Tc_2Cl_4(PR_3)_4$ (PR_3 = PEt_3, PMe_2Ph, $PMePh_2$) react with molten formamidine to produce mixtures of tris- and tetrakis-bridged formamidinate complexes of ditechnetium (eq 1). The displacement of chloride and

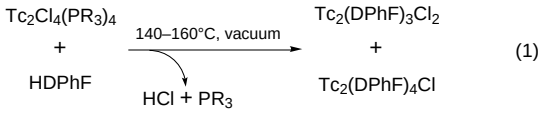

(1)

phosphine by $[DPhF]^-$ (diphenylformamidinate), however, was accompanied by the oxidation of the dimetal core from Tc^{II}_2 to $Tc^{II}Tc^{III}$ to produce the mixed-valent complexes $Tc_2(DPhF)_3Cl_2$ (**1**) and $Tc_2(DPhF)_4Cl$ (**2**) in low to moderate yield. While oxidation of a dimetal unit by formamidine is unusual, it is not unique. In the preparation of $Mo_2(DTolF)_4$ from $Mo(CO)_6$ for example, Mo(0) is oxidized by 2 electrons to Mo(II).[10] The oxidation of the dimetal core from Tc^{II}_2 to $Tc^{II}Tc^{III}$ probably occurs at the expense of the formamidine. At exactly what point the oxidation takes place along the reaction pathway is unclear.

Similar reactions have also been carried out with HDTolF, but the yields were invariably lower due to the increased solubility of the metal formamidinate products and the resulting difficulty encountered in separating the products from unreacted formamidine and reaction side products. The product distribution is evidently dependent on a number of variables including temperature, reaction time and the amount of excess ligand present. Higher temperatures and longer reaction times tended to favor the formation of **2**, although **1** was always present as a minor byproduct. The use of different phosphine precursors had a negligible effect on the product distributions and yield. These considerations notwithstanding, yields of only 51% and 20% have been achieved for **1** and **2**, respectively. Suffice it to say, there are probably other routes to **2** that will prove more efficient.

Currently, we are trying to improve and extend the use of $M_2Cl_4(PR_3)_4$ type compounds as precursors for other metal−metal multiply bonded complexes. Indeed, we have recently found that $Re_2(DPhF)_3Cl_3$ and $Re_2(DPhF)_4Cl_2$ can be prepared in moderate yields by the reaction of $Re_2Cl_4(PEt_3)_4$ with HDPhF.[31] We expect that this methodology will furnish an alternate route to $W_2(DPhF)_xCl_y$ type compounds and may ultimately provide a clean method for the preparation of quadruply bonded mixed Mo−W formamidinate complexes through the use of $MoWCl_4(PMePh_2)_4$ as a precursor.[32]

(26) (a) Slater, J. C. *Quantum Theory of Molecules and Solids*; McGraw-Hill: New York, 1974; Vol. 4. (b) Johnson, K. H. *Annu. Rev. Phys. Chem.* **1975**, *26*, 39. (c) Johnson, K. H. *Adv. Quantum Chem.* **1973**, *7*, 143.
(27) Herman, F.; Skillman, S. *Atomic Structure Calculations*; Prentice-Hall: Englewood Clifts, NJ, 1963.
(28) Norman, J. G., Jr. *Mol. Phys.* **1976**, *31*, 1191.
(29) Schwarz, K. *Phys. Rev. B*, **1972**, *5*, 2466.
(30) For example see: (a) Cotton, F. A.; Kim, Y.; Yokochi, A. *Inorg. Chim. Acta* **1995**, *236*, 55. (b) Cotton, F. A.; Ren, T.; Eglin, J. L. *J. Am. Chem. Soc.* **1990**, *112*, 3439. (c) Chakravarty, A. R.; Cotton, F. A.; Tocher, D. A. *Inorg. Chem.* **1985**, *24*, 1334.
(31) Cotton, F. A.; Haefner, S. C. Unpublished results

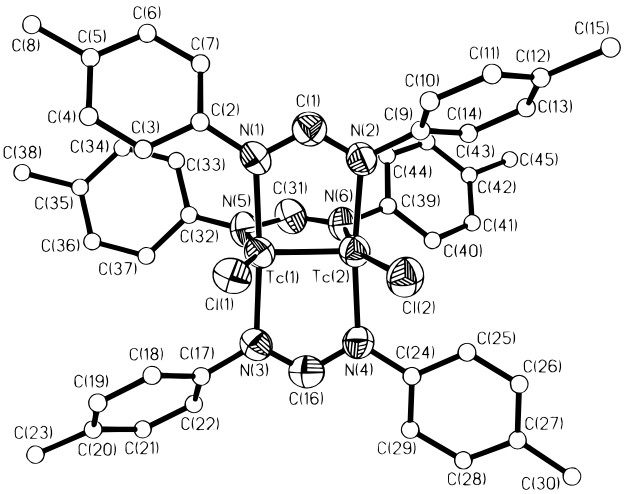

Figure 2. Structural diagram depicting $Tc_2(DTolF)_3Cl_2$ (**1a**). Thermal displacement ellipsoids are shown at the 50% probability level. For clarity, the carbon atoms of the tolyl groups are shown as spheres of arbitrary size.

Molecular Structures. The solid state molecular structures of $Tc_2(DTolF)_3Cl_2$, **1a**, and $Tc_2(DPhF)_4Cl{\cdot}C_7H_8$ (**2**$\cdot C_7H_8$) have been determined by single-crystal X-ray diffraction. A highly disordered molecule of crystallization precluded us from obtaining a satisfactory refinement for the structure of **1**.[33] We chose therefore to pursue the structure of the DTolF derivative, which was found to pose no unusual crystallographic problems. A structural drawing of $Tc_2(DTolF)_3Cl_2$ (**1a**) is presented in Figure 2. Complex **1a** approximates a pseudolantern geometry common among nearly all $M_2(L\text{-}L)_4$ type compounds. However, in the present case, the fourth bridging formamidinate ligand has been replaced by an equatorial chloride on each metal atom. The molecule maintains an essentially eclipsed conformation (torsion angle $\chi = 2.9$ [8]°) with the equatorial chlorides bound in a *syn* disposition. Although **1a** does not exhibit any crystallographic symmetry, the *syn* arrangement of the halides provides pseudo C_{2v} symmetry.

The metal−metal bond length of 2.0937 Å is quite short and is, in fact, among the shortest observed for a Tc−Tc metal bond. The only shorter Tc−Tc bond was that reported for the polymeric chain complex $[Tc_2Cl_6]_n^{2n-}$.[34,35] As evidenced by the nearly linear N(1)−Tc(1)−N(3) and N(1)−Tc(1)−N(3) bond angles, the equatorial chlorides do not impose any unusual steric demands upon the molecule. While the six Tc−Tc−N angles of the three formamidinate ligands are very close to 90°, the Tc−Cl bonds are distinctly swept back away from the center of the molecule with Tc−Tc−Cl angles of 108.80(4) and 107.94(3)°. The observed deformations are a consequence of the short Tc−Tc multiple bond and are not uncommon among compounds that contain equatorial monodentate ligands. By way of comparison, the average Tc−Tc−Cl angle in $[(n\text{-}Bu)_4N]_2[Tc_2Cl_8]$ is 103.66(6)°.[36] The Tc−Cl bond distances of 2.357(1) and 2.346(1) Å are similar to those found for the equatorial chloride ligands in the $Tc^{II}Tc^{III}$ compounds $[Tc_2Cl_4(PMe_2Ph)_4]^+$, $Tc_2Cl_5(PMe_2Ph)_3$, and $[Tc_2Cl_8]^{3-}$ (average Tc−Cl = 2.333[2], 2.344[3], and 2.364[8] Å, respectively).[37]

Recently, complexes of the type $M_2(DPhF)_3$ have been prepared for metals of the first transition series.[38] The presence of only three formamidinate ligands spanning two second or third row transition metals has been reported only once.[39] However, the compound $Mo_2(DPhF)_3Cl_2$ has recently been prepared in this laboratory.[40] More generally, dinuclear complexes with odd numbers of any kind of bridging ligand are rare.[2,41]

The novel structural nature of $Tc_2(DTolF)_3Cl_2$ lends itself to the opportunity for additional reactivity studies. Typically such lantern-type complexes with four bridging ligands react via initial attack at the more accessible axial positions. Replacement of one of the bridging ligands with two chloride ions creates the opportunity for chemistry to occur directly at the metal−metal bond. Removal of the equatorial chloride ligands is expected to open up one face of the dinuclear unit and provide direct access to the metal−metal bond. The remaining three formamidinate bridges would then help support the dimetal unit and prevent fragmentation into mononuclear species. One may envisage removal of one or both of the Cl groups through either halide abstraction techniques or direct M(0) reduction. In the absence of a suitable ligand, this may afford a coordinatively unsaturated and hence highly reactive $Tc_2(DPhF)_3^{n+}$ ($n = 0$, 1 or 2) type species. We are currently examining this possibility.

The structure of **2** consists of four bridging formamidinate ligands in the traditional lantern motif (Figure 3). The molecule resides on a crystallographic 4-fold axis which is colinear with the Tc−Tc bond. The chloride ion occupies an axial position along the 4-fold axis at a rather short distance of 2.450(4) Å from Tc(2). The Tc−Tc bond distance of 2.119(2) Å does not vary significantly from those reported for other $Tc^{II}Tc^{III}$ compounds and is characteristic of a metal−metal multiple bond between the technetium atoms.[1,2] The Tc−Tc bond length is, however, 0.03 Å longer than that found for **1a**. The difference in bond length is attributed to the relatively strong axial ligation by the chloride ion. The formation of the axial Tc−Cl bond effectively competes with the Tc−Tc σ-bonding thereby weakening the metal−metal bond.

Despite the presence of a partial δ bond, the two TcN_4 fragments are twisted from an eclipsed conformation by 12.8(2)°. The degree of twisting becomes quite apparent when the molecule is viewed down the Tc−Tc bond (Figure 4). Other dimetallic tetrakis(formamidinate) compounds range from those

(32) (a) Luck; R. L.; Morris, R. H. *J. Am. Chem. Soc.* **1984**, *106*, 7978. (b) Luck, R. L.; Morris, R. H.; Sawyer, J. F. *Inorg. Chem.* **1987**, *26*, 2432. (c) Cotton, F. A.; Falvello, L. R.; James, C. A.; Luck, R. L. *Inorg. Chem.* **1990**, *29*, 4759. (d) Cotton, F. A.; Eglin, J. L.; James, C. A. *Inorg. Chem.* **1993**, *32*, 681.

(33) $Tc_2(DPhF)_3Cl_2{\cdot}$solvent crystallized in the monoclinic space group *C*2/*c* (No. 15) with unit cell parameters $a = 9.672(2)$ Å, $b = 17.092(1)$ Å, $c = 23.305(3)$ Å, $\beta = 91.897(7)°$, $V = 3850.7$ (9) Å^3, $Z = 4$. The Tc−Tc bond length is 2.084(5) Å.

(34) (a) Cotton, F. A.; Daniels, L. M.; Falvello, L. R.; Grigoriev, M. S.; Kryuchkov, S. V. *Inorg. Chim. Acta* **1991**, *189*, 53. (b) Kryuchkov, S. V.; Grigoriev, M. S.; Kuzina, A. F.; Gulev, B. F.; Spitsyn, V. I. *Dokl. Akad. Nauk. SSSR* **1986**, 389; *Dokl. Chem.* **1986**, 147.

(35) The proposed structure of $[(C_5Me_5)Tc(\mu\text{-}O)_3Tc]_n$, whose Tc−Tc seperation was previously reported to be 1.867(4) Å (Kanellakopulos, B.; Nuber, B.; Raptis, K.; Ziegler, M. L. *Angew. Chem., Int. Ed. Engl.* **1989**, *28*, 1055), has been unambigously shown to be that of $(C_5Me_5)\text{-}ReO_3$: Burrell, A. K.; Cotton, F. A.; Daniels, L. M.; Petricek, V. *Inorg. Chem.* **1995**, *34*, 4253.

(36) Cotton, F. A.; Daniels, L. M.; Davison, A.; Orvig, C. *Inorg. Chem.* **1981**, *20*, 305.

(37) Cotton, F. A.; Shive, L. W. *Inorg. Chem.* **1975**, *14*, 2032.

(38) (a) Cotton, F. A.; Daniels, L. M.; Falvello, L. R.; Murillo, C. A. *Inorg. Chim, Acta.* **1994**, *219*, 7. (b) Cotton, F. A.; Daniels, L. M.; Falvello, L. R.; Maloney, D. J.; Matonic, J. H.; Murillo, C. A. *Inorg. Chim. Acta*, in press.

(39) Piriano, P.; Bruno, G.; Nicolo, F.; Faraone, F.; Lo Schiavo, S. *Inorg. Chem.* **1985**, *24*, 4760.

(40) Cotton, F. A.; Jordan, G. T., IV; Murillo, C. A.; Su, J. *Polyhedron*, in press.

(41) For other examples of complexes with odd numbers of polyatomic bridging ligands see: (a) Anderson, L. B.; Cotton, F. A.; Falvello, L. R.; Harwood, L. R.; Lewis, D.; Walton, R. A. *Inorg. Chem.* **1986**, *25*, 3637. (b) Bartley, S. L.; Bernstein, S. N.; Dunbar, K. R. *Inorg. Chim. Acta* **1993**, *213*, 213. (c) Cayton, R. H.; Chisholm, M. H.; Huffman, J. C.; Lobkovsky, E. B. *J. Am. Chem. Soc.* **1991**, *113*, 8709.

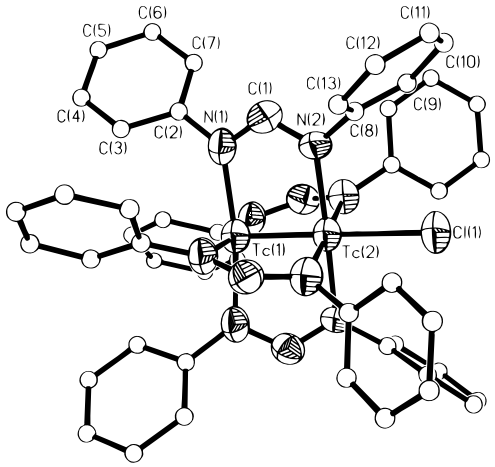

Figure 3. Drawing of $Tc_2(DPhF)_4Cl$ (**2**). Thermal displacement ellipsoids are shown at the 50% probability level. For clarity, the carbon atoms of the phenyl groups are shown as spheres of arbitrary size.

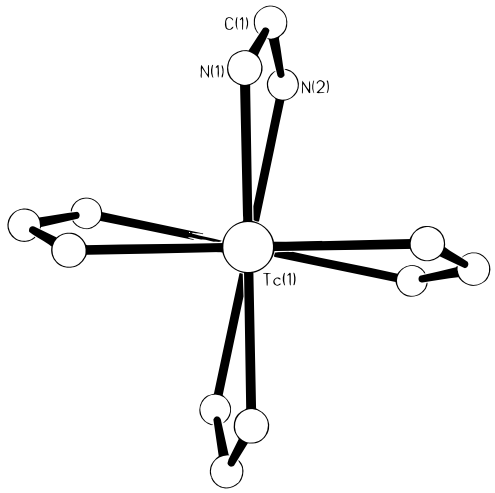

Figure 4. $Tc_2(DPhF)_4Cl$ (**2**) viewed along the Tc−Tc bond. The phenyl groups have been omitted for clarity.

that are rigorously eclipsed, as in the case of $Re_2(DTolF)_4Cl_2$,[14] to those that are dramatically twisted, as in the case of $Ni_2(DTolF)_4^+$ ($\chi = 27.4°$).[9] Although some relationship exists between the M−M torsion angle and bond order, packing considerations also appear to play a role.[42]

As a result of the axial chloride ion bound to Tc(2), the geometries around the two Tc centers are quite disparate. The coordination geometry around Tc(1) approximates that of a square pyramid with the second Tc atom occupying the apical position. Tc(1) resides approximately 0.16 Å above the plane defined by the four nitrogen atoms of the bridging formamidines. In contrast, Tc(2) lies at the center of a pseudooctahedron described by the four nitrogen atoms, the axial chloride ion, and Tc(1). The deviation of Tc(2) from the N_4 plane is negligible. More significant is the lengthening of the Tc(2)−N(2) bond distance by 0.07 Å relative to the Tc(1)−N(1) distance.

Compund **2** exists as discrete molecules, with no Tc−Cl−Tc bridging such as that found in $Tc_2(hp)_4Cl$ (hp = *o*-hydroxypyridinate), where there are infinite linear chains with symmetrical Cl^- bridges between the $[Tc_2(hp)_4]^+$ units.[43] The reason is fairly obvious; in $Tc_2(hp)_4Cl$, the axial positions of the neighboring cations can approach one another closely enough to allow the bridges to form. In **2**, the four phenyl groups project from each end of the $[Tc_2(DPhF)_4]^+$ cation making such an approach impossible. Instead each Cl^- approaches one Tc atom of each cation, in this case Tc(2), closely, and nestles into the bowl-like environment provided by the four phenyl groups. It is interesting that the Cl atom is not so completely sequestered as to permit disordered packing of the $Tc_2(DPhF)_4Cl$ molecules with themselves or with guest $Tc_2(DPhF)_4$ molecules, whereas it has been observed that $Tc_2(DTolF)_4Cl$ will act as host for $Tc_2(DTolF)_4$.[44]

Electronic Structures. In order to acquire a better understanding of the bonding involved in these metal−metal bonded systems theoretical calculations were performed on the model complexes $Tc_2(HNCHNH)_3Cl_2$ (**1m**) and $Tc_2(HNCHNH)_4Cl$ (**2m**). The results of the spin restricted SCF−Xα−SW calculations are presented in Tables 4 and 5. Included are the upper valence orbital energies, the relative charge in each atomic sphere, as well as the percent angular contributions of the metal atoms to each molecular orbital. The lowest-lying valence orbitals consist primarily of unperturbed C−H, N−H, C−N σ bonding orbitals and chlorine 3s lone pairs and are therefore excluded from the tables. The orbitals listed in Tables 4 and 5 are readily divided into three categories on the basis of the percent metal contribution. Orbitals that contain little or no metal character are primarily ligand π orbitals on the nitrogen atoms or are lone pair orbitals of the chlorine atoms. Metal−ligand bonding orbitals are those orbitals that exhibit up to 45% metal character. The third group, which is of primary interest in this discussion, are those orbitals that contain significant (> 49%) metal character; these may be described as metal−metal bonding and antibonding orbitals.

The ordering of the M−M molecular orbitals for both **1m** and **2m** is qualitatively the same as that found for $[Tc_2Cl_8]^{3-}$ and $[Mo_2(HNCHNH)_4]^+$.[45] For $Tc_2(HNCHNH)_4Cl$, the ordering is as follows: $7a_1$ (σ) < 7e (π) < $3b_2$ (δ) < $4b_2$ (δ^*) < 12e (π^*) < $11a_1$ (σ^*). For $Tc_2(HNCHNH)_3Cl_2$, the replacement of one formamidinate ligand by two equatorial chloride ligands has reduced the molecular symmetry from C_{4v} to C_{2v}. Under C_{2v} symmetry, the two sets of Tc−Tc π and π^* orbitals (e symmetry) are no longer degenerate and are split into sets of π_{xz} and π_{yz} bonding orbitals ($a_1 + b_1$ symmetry) and π_{xz}^* and π_{yz}^* antibonding orbitals ($b_2 + a_2$ symmetry). However, despite the non-degeneracy, the ordering of the M−M molecular orbitals remains unchanged, namely, $8a_1$ (σ) < $10a_1$ (π_{xz}) < $6b_1$ (π_{xy}) < $9b_1$ (δ) < $7a_2$ (δ^*) < $8a_2$ (π_{xy}^*) < $11b_2$ (π_{xz}^*) < $12b_2$ (σ^*). For purposes of comparison, the relative ordering of the molecular orbital energy levels for **1m** and **2m** are shown in Figure 5.

In both instances the highest occupied molecular orbital is the Tc−Tc δ^* orbital. The relative ordering of the δ^* and π^* orbitals is opposite of that found for $Re_2(HNCHNH)_4Cl_2$, $Re_2(HNCHNH)_4$, $Ru_2(HNCHNH)_4$, $Ru_2(HNNNH)_4$, and $Os_2(HNCHNH)_4Cl_2$.[46] In these examples, the π^* orbital was determined to be significantly lower in energy than the δ^* orbital. In complexes such as **2m**, the δ^* orbitals strongly interact with the nitrogen pπ-lone pairs of the ligand, resulting in the formation of bonding and antibonding pairs of orbitals. For $Tc_2(HNCHNH)_4Cl$, the pair of bonding and antibonding orbitals correspond to the $4b_2$ and $2b_2$ molecular orbitals. It is precisely this antibonding interaction between the δ^* and N−pπ

(42) (a) Agaskar, P. A.; Cotton, F. A.; Dunbar, K. R.; Falvello, L. R.; Tetrick, S. M.; Walton, R. A. *J. Am. Chem. Soc.* **1986**, *108*, 4850. (b) Cotton, F. A.; Dunbar, K. R.; Matusz, M. *Inorg. Chem.* **1986**, *25*, 3641.

(43) Cotton, F. A.; Fanwick, P. E.; Gage, L. D. *J. Am. Chem. Soc.* **1980**, *102*, 1570.

(44) Cotton, F. A.; Haefner, S. C.; Sattelberger, A. P. Unpublished results.

(45) Cotton, F. A.; Kalbacher, B. L. *Inorg. Chem.* **1977**, *16*, 2386.

(46) Cotton, F. A.; Feng, X. *Inorg. Chem.* **1989**, *28*, 1180.

Table 4. Upper Valence Molecular Orbitals for $Tc_2(HNCHNH)_4Cl$ (**2m**)

			% contribution									Tc angular contribution		
C_{4v} level	Tc−Tc orbital	energy (eV)	Tc1	Tc2	Cl	4 N1	4 N2	4 C	4 H_{N1}	4 H_{N2}	4 H_C			
$9b_1$		−2.807	58	0	0	36	1	1	1	0	2			100% d
$11a_1$	σ^*	−3.859	33	45	8	5	7	1	0	1	0	1% s	25% p	74% d
$8b_1$		−4.069	1	60	0	0	34	1	0	2	1			
12e	π^*	−6.351	47	46	3	2	1	1	0	0	0			100% d
$4b_2$	δ^*	−6.522	35	23	0	22	20	0	0	0	0			100% d
$2a_2$		−7.496	0	0	0	50	50	0	0	0	0			
11e		−7.939	0	0	1	51	48	0	0	0	0			
$3b_2$	δ	−8.493	35	44	0	2	7	11	0	0	0			100% d
$10a_1$		−8.813	17	8	64	5	2	1	1	0	1	29% s	1% p	70% d
10e		−8.941	9	1	29	22	23	5	2	1	7			
9e		−9.128	5	2	57	23	3	3	1	0	4			
$2b_2$		−10.150	24	32	0	20	23	0	0	0	0			100% d
8e		−10.399	3	10	4	24	47	1	2	7	0			
$9a_1$		−10.664	10	11	18	22	16	9	2	2	11			
$1a_2$		−10.740	0	0	0	33	34	33	0	0	0			
7e	π	−10.998	35	39	4	9	6	5	1	0	0			100% d
6e		−11.274	9	11	0	25	29	24	0	0	1			
$7b_1$		−11.994	22	19	0	15	13	12	2	1	15			100% d
$8a_1$		−12.201	10	13	0	27	37	1	4	7	0			
$1b_2$		−12.328	15	11	0	30	24	19	0	0	0			100% d
$6b_1$		−12.868	18	20	0	24	27	0	4	6	0			100% d
$7a_1$	σ	−13.672	41	43	7	2	1	3	0	0	3	4% s	6% p	89% d

Table 5. Upper Valence Molecular Orbitals for $Tc_2(HNCHNH)_3Cl_2$ (**1m**)

			% contribution										Tc angular contribution		
C_{2v} level	Tc−Tc orbital	energy (eV)	2 Tc	2 Cl	2 N_x	4 N_y	C_x	2 C_y	2 H_{Nx}	4 H_{Ny}	H_{Cx}	2 H_{Cy}			
$13b_2$		−2.854	67	9	5	17	0	0	0	1	0	0		1% p	99% d
$15a_1$		−2.983	57	10	11	17	0	1	1	1	1	1	1% s	1% p	98% d
$12b_2$	σ^*	−3.933	85	6	7	0	0	0	1	0	0	0		11% p	89% d
$11b_2$	π_{xz}^*	−4.986	89	7	3	0	1	0	0	0	0	0		1% p	99% d
$8a_2$	π_{yz}^*	−5.418	95	1	0	3	0	1	0	0	0	0			100% d
$7a_2$	δ^*	−5.828	60	1	8	30	0	0	0	0	0	0			100% d
$6a_2$		−6.975	3	5	54	38	0	0	0	0	0	0			
$10b_2$		−7.231	0	4	1	93	0	0	0	0	0	0			
$9b_1$	δ	−7.463	70	19	1	3	3	4	0	0	0	0			100% d
$5a_2$		−8.178	10	60	18	11	0	0	0	0	0	0			
$14a_1$		−8.377	28	58	9	1	1	1	0	0	1	0		18% p	100% d
$9b_2$		−8.475	3	94	2	0	0	0	0	0	0	0			
$8b_1$		−8.492	10	24	1	46	1	7	0	4	0	7			
$13a_1$		−8.988	5	68	17	3	2	3	2	0	2	0			
$7b_1$		−9.097	9	43	1	31	0	9	0	2	0	4			
$8b_2$		−9.538	17	69	9	3	0	0	2	0	0	0	4% s	29% p	68% d
$4a_2$		−9.655	39	29	10	21	0	0	0	0	0	0		1% p	99% d
$12a_1$		−10.021	38	11	13	19	2	4	2	2	3	5	60% s	5% p	36% d
$3a_2$		−10.060	10	6	0	71	0	1	0	11	0	0			
$6b_1$	π_{yz}	−10.149	93	2	1	1	0	1	0	1	0	0			100% d
$5b_1$		−10.278	5	5	38	23	19	10	0	0	0	1			
$11a_1$		−10.498	2	7	1	61	0	27	0	0	0	0			
$10a_1$	π_{xz}	−10.813	71	21	1	3	0	1	0	0	0	1	2% s		98% d
$4b_1$		−11.516	25	5	22	29	8	10	0	0	0	0			100% d
$9a_1$		−11.535	40	13	11	13	4	6	1	2	5	7			100% d
$7b_2$		−11.541	21	8	44	14	1	0	8	3	0	0	37% s	4% p	60% d
$6b_2$		−12.259	35	2	9	42	0	0	2	9	0	0	2% s		97% d
$8a_1$	σ	−12.788	86	2	2	2	1	2	0	0	1	2	3% s	6% p	91% d

lone pairs that sufficiently destabilizes the δ^* orbital in the Re_2, Ru_2 and Os_2 systems and changes the ordering of the δ^* and π^* levels. In the present case the interaction between the δ^* and pπ lone pairs is not strong enough to push the δ^* orbital above the π^* orbital.

By comparing the relative orbital energies of **2m** with those of **1m** in Figure 5, we can further see the influence that the pπ lone pair orbitals of the formamidinate ligand have over the relative energy of the δ^* orbital. Replacement of one HNCHNH group with two chlorine atoms reduces the δ^*−pπ interaction which creates a larger energy difference between the δ^* ($7a_2$) and π_{yz}^* ($8a_2$) orbitals. It should be pointed out that under C_{2v} symmetry, the π_{yz}^* orbital has the correct symmetry to also interact with the formamidinate pπ lone pair orbitals, but the interaction is apparently negligible as judged by the insignificant percent contribution of the nitrogen atoms to the $8a_2$ orbital.

The calculations for both compounds predict a very small HOMO−LUMO separation ($\Delta E = 0.171$ and 0.410 eV). Thus, some thermal population of the LUMO (π^*) might be anticipated owing to the rather small energy difference between the orbitals. However, it has been found that the antibonding interaction between the δ^* and nitrogen pπ orbitals tends to be over estimated by a few tenths of an eV.[46,47] Therefore, the actual energy gap between the δ^* and π^* orbitals is likely to be larger. Furthermore, the Tc−Tc bond lengths for **1a** and **2**,

(47) Rizzi, G. A.; Casarin, M.; Tondello, E.; Piraino, P.; Grannozzi, G. *Inorg. Chem.* **1987**, *26*, 3406.

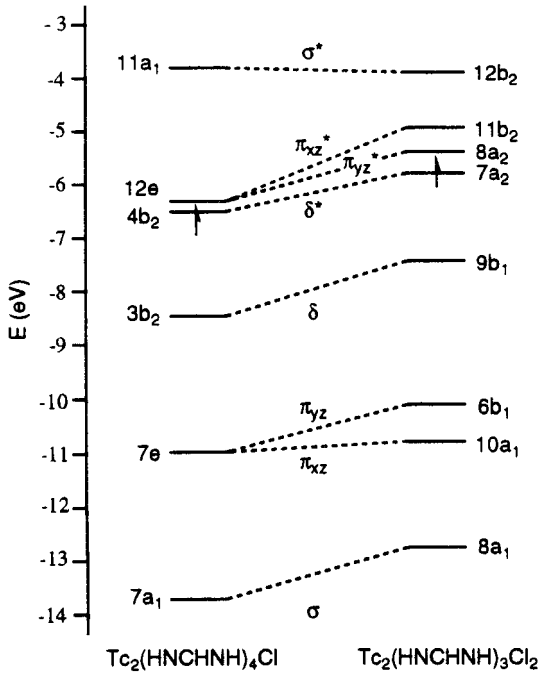

Figure 5. Upper valence molecular orbital diagrams for $Tc_2(HNCHNH)_4Cl$ and $Tc_2(HNCHNH)_3Cl_2$ calculated by the SCF−Xα−SW method. Only orbitals with significant metal−metal bond character are shown.

measured at room temperature, are in agreement with those found for other Tc_2^{5+} species in which a $\sigma^2\pi^4\delta^2\delta^*$ configuration has been unambiguously demonstrated.[2] The metal−metal bond should be noticeably elongated if there existed significant population of the π^* orbital. Clearly this is not the case for **1a** or **2**. In fact, the Tc−Tc bond length for **1a** is among the shortest reported for a Tc−Tc multiple bond.

Electrochemistry. Electrochemical studies of $Tc_2(DTolF)_3Cl_2$ and $Tc_2(DPhF)_4Cl$ were performed in CH_2Cl_2 using 0.1 M [*n*-Bu_4N][PF_6] as a supporting electrolyte. As anticipated, the cyclic voltammograms of **1** and **2** reveal rich redox behavior ubiquitous among metal−metal multiply bonded compounds. Both compounds undergo reversible one electron oxidation and reduction processes presumably producing the respective Tc_2^{6+} and Tc_2^{4+} species. The reduction from $Tc^{II}Tc^{III}$ to $Tc^{II}Tc^{II}$ occurs at $E_{1/2} = -1.5$ and -1.73 V vs Cp_2Fe for **1** and **2**. The reversibility of these couples demonstrate that, unlike $Ru_2(DTolF)_4Cl$,[11a] $Tc_2(DPhF)_3Cl_2$ and $Tc_2(DPhF)_4Cl$ are stable upon reduction with respect to chloride ion dissociation, at least over the time scale of the experiment. Likewise the reversibility of oxidation processes, which appear at -0.2 V and -0.46 V vs Cp_2Fe, for **1** and **2** indicate that the structural integrity of the molecules is retained upon oxidation.[48] Both redox processes for **2** occur at more negative potentials that those of **1.** This observation is in accord with the replacement of the two equatorial chlorides in favor of a fourth bridging DPhF ligand. The formamidinate ligand is much better at stabilizing the higher oxidations states than the two chloride atoms due to its greater π-basicity. Consequently, the tetrakis(formamidinate) complex **2** is more easily oxidized to Tc^{III}_2 and more difficult to reduce to Tc^{II}_2 than **1**.[18]

Comparison of the redox potentials of $Tc_2(DPhF)_4Cl$ with those associated with $Re_2(DTolF)_4Cl_2$ suggest that complexes of the type $[Re_2(DPhF)_4Cl]^n$ ($n = -1, 0, +1$) would be a more suitable target than either $[Re_2(DTolF)_4]^{n+}$ ($n = 0, 1, 2$) or $[Re_2(DTolF)_4Cl_2]^n$ ($n = 0, -1, -2$) for the preparation of a series of dirhenium compounds that differ in electronic configuration but maintain identical ligand sets. This is understandable when one takes into consideration that molecular species possessing a divalent charge, i.e. $[Re_2(DTolF)_4]^{2+}$ and $[Re_2(DTolF)_4Cl_2]^{2-}$, will be more susceptible to halide abstraction or dissociation. This point is demonstrated by the less than ideal redox behavior of $Re_2(DTolF)_4Cl_2$.[14] Furthermore, the associated redox couples for $Re_2(DPhF)_4Cl$ are likely to be more accessible than those for either $Re_2(DPhF)_4$ or $Re_2(DPhF)_4Cl_2$. These considerations, when taken together, illustrate the advantages of pursuing $Re_2(DPhF)_4Cl$ as a structural framework for building a series of complexes that maintain the same ligand environment but possess different electronic configurations.

Acknowledgment. This work was supported by the Laboratory Directed Research and Development Program at Los Alamos National Laboratory. The authors also acknowledge financial assistance from the National Science Foundation and the Laboratory for Molecular Structure and Bonding for support of the facilities at Texas A&M University. The authors thank Dr. Robert Hightower (Oak Ridge National Laboratory) for a generous gift of ammonium pertechnetate. We are indebted to Dr. Xuejun Feng for his advice and assistance with the theoretical calculations.

Supporting Information Available: Two X-ray crystallographic files in CIF format are available in electronic form only via the Internet. See any current masthead page for ordering information.

IC960535M

(48) Surprisingly, attempts to oxidize **1** with [Cp_2Fe][PF_6] led to the isolation of $Tc_2(DPhF)_3Cl_2F$, which possesses an axial fluoride ion bound to one of the technetium atoms. Evidently the oxidation product is sufficiently electrophilic to abstract a fluoride ion from $[PF_6]^-$: Cotton, F. A.; Haefner, S. C.; Sattelberger, A. P. Unpublished results.